Analytical solutions for von Kármán streets of hollow vortices

Darren G. Crowdy and Christopher C. Green

Related Articles

Additional information on Phys. Fluids

Analytical solutions for von Kármán streets of hollow vortices

Darren G. Crowdy[a)] and Christopher C. Green[b)]

Department of Mathematics, Imperial College London, 180 Queen's Gate, London SW7 2AZ, United Kingdom

New analytical solutions are presented for steadily translating von Kármán vortex streets made up of two infinite rows of hollow vortices. First, the solution for a single row of hollow vortices due to Baker *et al.* ["Structure of a linear array of hollow vortices of finite cross-section," J. Fluid Mech. **74**, 469 (1976)] is rederived, in a modified form, and using a new mathematical approach. This approach is then generalized to find relative equilibria for both unstaggered and staggered double hollow vortex streets. The method employs a combination of free streamline theory and conformal mapping ideas. The staggered hollow vortex streets are compared with analogous numerical solutions for double streets of vortex patches due to Saffman and Schatzman ["Properties of a vortex street of finite vortices," SIAM (Soc. Ind. Appl. Math.) J. Sci. Stat. Comput. **2**, 285 (1981)] and several common features are found. In particular, within the two different inviscid vortex models, the same street aspect ratio of approximately 0.34–0.36 is found to have special significance for the equilibria. © *2011 American Institute of Physics*. [doi:10.1063/1.3665102]

I. INTRODUCTION

The formation of a train of alternating vortices, commonly known as a von Kármán vortex street, in the wakes of flows past an obstacle has been a topic of enduring interest in fluid mechanics. The monograph by Saffman[1] discusses these vortex structures in the inviscid limit, while Williamson[2] has given a more general review of the subject. The name of these vortex street structures hails from the first theoretical studies of them, due to von Kármán and Rubach,[3] and von Kármán[4] in which arrays of point vortices are used to model the centres of vorticity. This approximate approach has been very successful but has several limitations, among which are the difficulties in fitting the model to the wake behind bluff bodies owing to the infinite kinetic energy associated with them.[2] Within the point vortex model, an interesting fact, that has been used extensively in the literature, is that only when the aspect ratio κ of the street is equal to $\sinh^{-1}(1)/\pi \approx 0.28055$ is the configuration neutrally stable to linear disturbances. In laboratory experiments of vortex shedding by blunt bodies, the aspect ratio is actually found to depend on the shape of the object, the characteristics of the flow, and the distance downstream. Structures resembling vortex streets, and with broadly similar aspect ratios, are also observed to form in the atmosphere and ocean.[5–7]

New applications and manifestations of these vortex street structures arise constantly and in different areas of physics. In studies of fish schooling, it has been found that fish often weave through a wake to let each oncoming vortex pass it on the same side as a thrust wake vortex would, a phenomenon that has been christened the *Kármán gait*.[11] Most recently, it has been proposed that the efficiency of wind farms can be enhanced by arranging vertical axis turbines in configurations reminiscent of the vortex distribution usually associated with staggered von Kármán vortex streets.[12] Shao *et al.*[8] have employed a von Kármán vortex street to pattern catalysts and successfully grow silicon nanowire arrays with a disk-like superstructure. It has also been observed experimentally that long-lived alternately aligned vortex pairs, reminiscent of the classical von Kármán vortex streets, are formed in the wake of an obstacle potential moving in a Bose-Einstein condensate.[9,10] Given all these applications, a thorough theoretical understanding of these vortex structures is important.

Since von Kármán's early work, several more realistic theoretical models have been investigated. Hooker[13] and Schaefer and Eskinazi[14] have studied the effects of viscosity on the vortex street structure by considering models consisting of a direct superposition of Lamb monopoles. Saffman and Schatzman,[15] on the other hand, focussed on inviscid models and had the idea of regularizing von Kármán's point vortices by replacing them with finite-area vortex patches. By making use of technical advantages afforded by the vortex patch model in the absence of viscosity, they found numerical solutions for steadily translating double vortex streets and studied their structure and stability[16] (see also subsequent contributions by Kida[17] and Meiron *et al.*[18]). Even with today's computational power, the numerical determination of steady double streets of finite-area vortex patches is a challenging undertaking.

From a theoretical viewpoint, it would be convenient to have available an analytical solution for inviscid double vortex street structures involving finite-area vortices that can be readily evaluated. The purpose of this paper is to present what are believed to be the first such solutions. Instead of the point vortex model or the vortex patch model employed by Saffman and Schatzman,[15] here, we model each vortex as a so-called hollow vortex, defined to be a finite-area vortex, bounding a constant pressure region, with a boundary that is a vortex sheet. A review by Saffman[24] gives interesting perspectives as to the advantages and drawbacks of these various vortex

a)Electronic mail: d.crowdy@imperial.ac.uk.
b)Electronic mail: christopher.c.green05@imperial.ac.uk.

models. Our work can be viewed as the double street generalization of the study by Baker *et al.*[19] who identified an analytical solution for a single row of hollow vortices. Baker[20] went on to study the energetics of this solution class, while later work by Ardalan *et al.*[21] looked at the effects of compressibility. A classical solution for hollow vortices is due to Pocklington[22] who produced analytical solutions, in terms of elliptic functions, for a co-travelling hollow vortex pair; Moore and Pullin[35] extended this to the compressible vortex pair (see also Leppington[36]). Llewellyn Smith and Crowdy[33] have recently presented new exact solutions for isolated hollow vortex equilibria in ambient irrotational straining flows. Other work on constructing hollow vortex equilibria in the wakes of bluff bodies has recently been contributed by Telib and Zannetti.[23]

The main result of this paper can be stated simply: we demonstrate that a conformal mapping from the annulus $\rho < |\zeta| < 1$ in a parametric ζ-plane to the fluid region in a principal period window exterior to two typical hollow vortex members in a steadily translating street is given by the explicit formula

$$z(\zeta) = \int_{\zeta_0}^{\zeta} \left\{ \frac{B P^2(\zeta'\overline{\gamma_1}, \rho) P^2(\zeta'\overline{\gamma_2}, \rho)}{P(\zeta'/\alpha, \rho) P(\zeta'\overline{\alpha}, \rho) P(\zeta'/\beta, \rho) P(\zeta'\overline{\beta}, \rho)} \right\} d\zeta', \tag{1}$$

where the special function $P(\zeta, \rho)$ is defined by

$$P(\zeta, \rho) \equiv (1 - \zeta) \prod_{k=1}^{\infty} (1 - \rho^{2k}\zeta)(1 - \rho^{2k}\zeta^{-1}). \tag{2}$$

There are complementary formulae, given herein, that determine the associated flow fields. For appropriate choices of the parameters in Eq. (1), the formula encompasses both unstaggered and staggered vortex streets. In this paper, we identify only solutions in which the sizes of all vortices in the two rows making up the street are the same. The parameters in Eq. (1) are then uniquely determined by specifying the translational speed of the street configuration and the vortex size.

This paper documents the construction of the steady state equilibria and shows how to arrive at formula (1). Ongoing work exploring the important question of their stability will be reported on elsewhere.

II. SINGLE ROW OF HOLLOW VORTICES

It is expedient to first rederive the solution for a single row of hollow vortices due to Baker *et al.*[19] using a mathematical approach that differs from the original derivation.

Let the centroids of the hollow vortices, in a complex $z = x + iy$ plane, be at $x = nL$ where n is any integer and L is the period of the arrangement. By the periodicity of the row, it is enough to consider a single period window. The notation ∞^+ is used to denote the region of the period window as $y \to +\infty$, while ∞^- denotes the region as $y \to -\infty$. See Figure 1.

The construction will proceed using conformal mapping. Let the unit ζ-disc be transplanted, by the conformal map $z(\zeta)$, to a single period window of the vortex row containing

a single hollow vortex. Since the boundary of the hollow vortex is unknown *a priori*, the challenge is to find the functional form of this conformal mapping; mathematically, this is a free boundary problem.

We must ensure that the function $z(\zeta)$ is L-periodic in the x-direction. The boundary of the hollow vortex is the image of the unit circle $|\zeta| = 1$ under the map $z(\zeta)$, and it should be noted that traversing $|\zeta| = 1$ in an anticlockwise sense corresponds to traversing the boundary of the hollow vortex in a clockwise sense. Two points inside the unit disc, denoted α and β, will be taken to map to ∞^+ and ∞^-, respectively. Since we require $z(\zeta)$ to jump by L as the point α is encircled in a positive sense, then, we require that, near $\zeta = \alpha$,

$$z(\zeta) = -\frac{iL}{2\pi} \log(\zeta - \alpha) + \text{analytic function}. \tag{3}$$

Similarly, near $\zeta = \beta$, we require that

$$z(\zeta) = \frac{iL}{2\pi} \log(\zeta - \beta) + \text{analytic function}. \tag{4}$$

To uniquely define $z(\zeta)$, it is necessary to specify a choice of branch cut joining the two logarithmic branch points at $\zeta = \alpha$ and β. This is done later.

The approach of this paper is to exploit ideas from free streamline theory[26,27] where the problem is solved by finding separate expressions for the complex potential and the complex velocity; then, the functional form of the conformal mapping follows from the chain rule.

A. Circular slit mapping

An important tool in the following analysis is the circular slit mapping:

$$\eta(\zeta; \gamma) \equiv \frac{\omega(\zeta, \gamma)}{|\gamma| \omega(\zeta, 1/\overline{\gamma})}, \tag{5}$$

where $|\gamma| < 1$ and

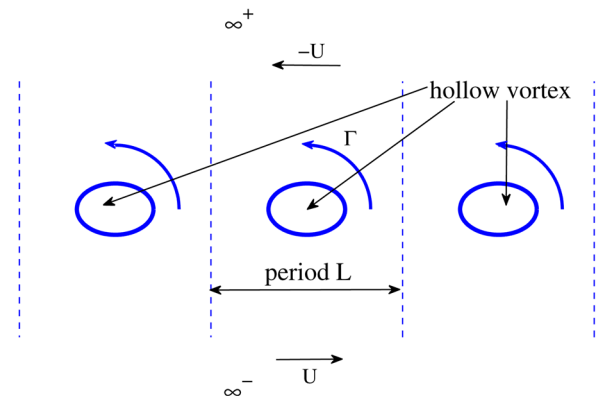$$\omega(\zeta, \gamma) = (\zeta - \gamma). \tag{6}$$

FIG. 1. (Color online) Three periods of a period-L row of hollow vortices. The shape of the vortex sheet bounding the hollow region is to be determined.

The function $\eta(\zeta; \gamma)$ clearly has a simple zero at $\zeta = \gamma$. It is straightforward to verify that $|\eta(\zeta; \gamma)|$ is constant on $|\zeta| = 1$, so the unit ζ-circle maps onto the unit circle in a complex η-plane. Since $\eta(\zeta; \gamma)$ is a Möbius map, it follows that the unit ζ-disc maps in a one-to-one fashion onto the unit disc in a complex η-plane with $\zeta = \gamma$ mapping to $\eta = 0$.

B. The function *w(z)*

Let the complex potential for the potential flow associated with the vortex row be denoted $w(z)$ and let the circulation around the hollow vortex be Γ. This means that $w(z)$ must change by Γ as a single anticlockwise circuit around the vortex is made. As $z \to \infty^\pm$, we require

$$w(z) \sim \mp Uz \tag{7}$$

for some U to be determined. The boundary of the hollow vortex must be a streamline so

$$\text{Im}(w(z)) = \text{constant}, \quad \text{on } |\zeta| = 1. \tag{8}$$

If we introduce the function,

$$W(\zeta) = w(z(\zeta)), \tag{9}$$

it follows from Eqs. (3) and (4) that,

$$\begin{aligned} W(\zeta) &\sim \frac{iLU}{2\pi} \log(\zeta - \alpha) \text{ as } \zeta \to \alpha, \\ W(\zeta) &\sim \frac{iLU}{2\pi} \log(\zeta - \beta) \text{ as } \zeta \to \beta. \end{aligned} \tag{10}$$

C. The function *dw/dz*

The boundary of the hollow vortex is a vortex sheet, and the pressure is constant inside it, so Bernoulli's theorem[25] implies that the fluid speed is constant on the vortex boundary. Hence,

$$\left| \frac{dw}{dz} \right| = \text{constant}, \quad \text{on } |\zeta| = 1. \tag{11}$$

By the symmetry of the configuration, we expect to have two stagnation points at the boundaries of the period window on the real axis. The complex velocity dw/dz must also be L-periodic.

D. Solutions in terms of circular slit mappings

In the complex ζ-plane, the logarithmic singularities (10) of $W(\zeta)$ have a physical interpretation as point vortices, of equal circulation, situated at $\zeta = \alpha$ and β. The function $W(\zeta)$ also satisfies the streamline condition on the boundary of the hollow vortex; it would satisfy the same condition if the hollow vortex is replaced by a solid body. It follows that an expression for $W(\zeta)$ can be determined either by application of the so-called Milne-Thomson circle theorem[26] or, alternatively, from the work of Crowdy and Marshall[28] where general analytical expressions are derived for the complex potentials associated with point vortices situated exterior to a collection of solid bodies. The result is

$$\begin{aligned} W(\zeta) &= \frac{iLU}{2\pi} \log \eta(\zeta; \alpha) + \frac{iLU}{2\pi} \log \eta(\zeta; \beta) \\ &= \frac{iLU}{2\pi} \log(\eta(\zeta; \alpha)\eta(\zeta; \beta)). \end{aligned} \tag{12}$$

In order that $w(z)$ changes by Γ as an anticlockwise circuit of the hollow vortex is made, it is necessary to pick

$$U = \frac{\Gamma}{2L}. \tag{13}$$

By the symmetry of the row configuration, it is natural to choose

$$\alpha = ia = -\beta, \tag{14}$$

where a is some real constant. Furthermore, we take the branch cut between the logarithmic branch points at $\pm ia$ to be along the imaginary axis, with the two sides of this cut mapping to the two sides of the period window. The centre of this cut, located at $\zeta = 0$, then maps to the two points at the edges of the period window along the x-axis. See Figure 2. As just mentioned, we expect the latter points to be stagnation points of the flow.

With the choice of Eq. (14), Eq. (12) becomes

$$W(\zeta) = \frac{iLU}{2\pi} \log\left(\frac{\zeta^2 + a^2}{\zeta^2 + 1/a^2}\right). \tag{15}$$

Since dw/dz is analytic everywhere in the fluid region, with zeros only at the stagnation points, we deduce that

$$\frac{dw}{dz} = R\zeta, \tag{16}$$

where R is a complex constant. It is obvious that this has constant modulus on $|\zeta| = 1$ and a zero at $\zeta = 0$. Since $dw/dz \to -U$ as $\zeta \to ia$, we deduce that $R = iU/a$, so

$$\frac{dw}{dz} = \frac{iU\zeta}{a}. \tag{17}$$

It follows from the chain rule that

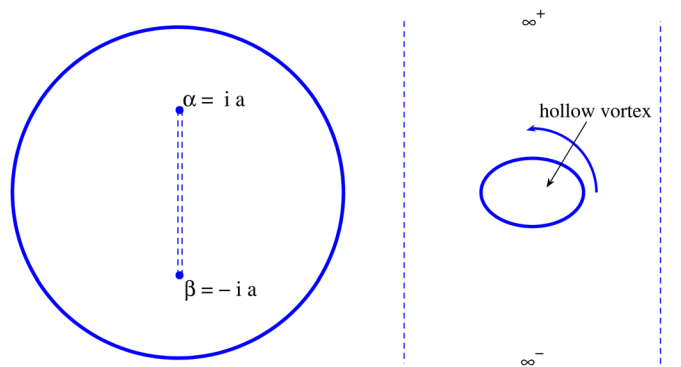FIG. 2. (Color online) The preimage unit ζ-disc with branch cut joining $\alpha = ia = -\beta$ (the preimages of ∞^+ and ∞^-) chosen along the imaginary ζ-axis and a typical period window of the vortex row. The circle $|\zeta| = 1$ maps to the hollow vortex boundary. The two sides of the branch cut map, under $z(\zeta)$, to the two edges of the period window.

$$\frac{dz}{d\zeta} = \frac{dW/d\zeta}{dw/dz} = \frac{dW/d\zeta}{iU\zeta/a} = \frac{aL}{\pi}\left[\frac{1}{\zeta^2 + a^2} - \frac{1}{\zeta^2 + 1/a^2}\right]. \quad (18)$$

On integration, the final map is found to be

$$z(\zeta) = \frac{L}{\pi}\left[\tan^{-1}(\zeta/a) - a^2\tan^{-1}(a\zeta)\right] + z_0, \quad (19)$$

where z_0 is a constant. For given L, the map (19) depends on the single parameter a, which reflects the size of each hollow vortex in the row. The solution (19) appears to be different to that found by Baker *et al.*[19] but is in fact equivalent, as shown in Appendix A.

III. HOLLOW VORTEX STREETS

The foregoing rederivation is useful because a direct generalization of it leads to solutions for vortex streets made up of two infinite rows of hollow vortices. Attention is restricted to solutions where the vortices in each row have identical shapes, with the area of the vortices in both rows being equal, but the method can, in principle, be readily generalized to find more general classes of solution. Both unstaggered and staggered street solutions will be examined.

Following the single row analysis, consider a conformal mapping from the annulus $\rho < |\zeta| < 1$ to a single period window of a vortex street in a complex z-plane. The circles $|\zeta| = \rho$ and $|\zeta| = 1$ map to the vortex sheets bounding the two hollow vortices in this representative period window and it should be noted that traversing $|\zeta| = 1$ in an anticlockwise sense corresponds to traversing the boundary of its image in a clockwise sense. As before, two interior points of the annulus, denoted α and β, will map to ∞^+ and ∞^-, respectively. Near $\zeta = \alpha$, we must have

$$z(\zeta) = -\frac{iL}{2\pi}\log(\zeta - \alpha) + \text{analytic function}, \quad (20)$$

and, near $\zeta = \beta$,

$$z(\zeta) = \frac{iL}{2\pi}\log(\zeta - \beta) + \text{analytic function}. \quad (21)$$

We must also make a choice of branch cut, interior to the annulus $\rho < |\zeta| < 1$, joining points α and β. The two sides of this branch cut will map to the two vertical sides of the principal period window of the configuration. By a rotational degree of freedom in the Riemann mapping theorem, α is taken to be real and positive. See Figure 3.

A. Circular slit mapping

It is again helpful to introduce a circular slit mapping. It is given by the same formula as in (5), i.e.,

$$\eta(\zeta; \gamma) \equiv \frac{\omega(\zeta, \gamma)}{|\gamma|\omega(\zeta, 1/\bar{\gamma})}, \quad (22)$$

where γ is a point in the annulus $\rho < |\zeta| < 1$, but now with

$$\omega(\zeta, \gamma) \equiv -\frac{\gamma}{C}P(\zeta/\gamma, \rho), \quad (23)$$

where

$$P(\zeta, \rho) \equiv (1 - \zeta)\prod_{k=1}^{\infty}(1 - \rho^{2k}\zeta)(1 - \rho^{2k}\zeta^{-1}),$$

$$C = \prod_{k=1}^{\infty}(1 - \rho^{2k})^2. \quad (24)$$

The function $P(\zeta, \rho)$ can be shown, directly from its infinite product definition, to satisfy the functional relations

$$P(\zeta^{-1}, \rho) = -\zeta^{-1}P(\zeta, \rho), \qquad P(\rho^2\zeta, \rho) = -\zeta^{-1}P(\zeta, \rho). \quad (25)$$

The function (22) has the useful property that

$$|\eta(\zeta; \gamma)| = \text{constant}, \quad \text{on } |\zeta| = \rho, 1. \quad (26)$$

Property (26) can be directly verified by making use of the relations (25).

It is worth pointing out that the functional form of $\eta(\zeta; \gamma)$ in Eq. (22) follows by invoking results on multiply connected slit mappings due to Crowdy and Marshall;[29] indeed, the function $\eta(\zeta; \gamma)$ maps the annulus $\rho < |\zeta| < 1$ to the unit disc in a complex η-plane containing an excised concentric circular slit. In the language of Ref. 29, the function $\omega(\zeta, \gamma)$ defined in Eqs. (23) and (24) is the so-called *Schottky-Klein prime function* associated with the annulus $\rho < |\zeta| < 1$.

B. The function *w(z)*

The street is expected to translate uniformly in the x-direction with speed U. Let the complex potential for the flow in a co-travelling frame be denoted by $w(z)$ and let the circulations around the two hollow vortices be $\pm\Gamma$. As $z \to \infty^{\pm}$, we require

$$w(z) \sim -Uz + \text{constant}. \quad (27)$$

The vortices will be stationary in the co-travelling frame and their boundaries will be streamlines so that
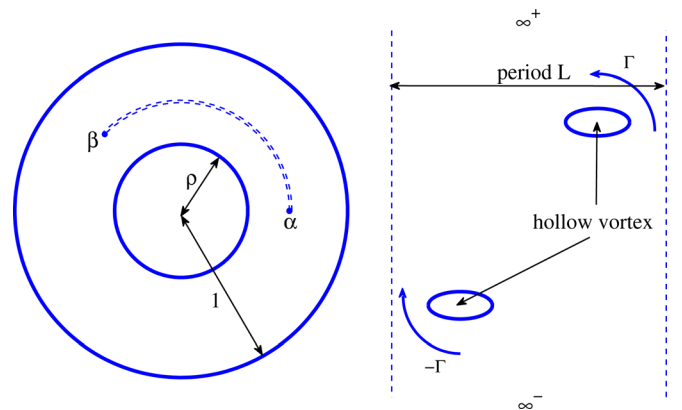

FIG. 3. (Color online) The preimage annulus $\rho < |\zeta| < 1$ and a typical period window of a hollow vortex street. The two sides of the branch cut joining α and β (the preimages of ∞^+ and ∞^-) are mapped by $z(\zeta)$ to the two edges of the period window. The two circles $|\zeta| = \rho$, 1 each map to one of the hollow vortex boundaries.

$$\text{Im}(w(z)) = \text{constant}, \quad \text{on } |\zeta| = \rho, 1. \tag{28}$$

If we introduce the function

$$W(\zeta) = w(z(\zeta)), \tag{29}$$

it follows from Eqs. (20) and (21) that

$$\begin{aligned} W(\zeta) &\sim \frac{iLU}{2\pi} \log(\zeta - \alpha) \text{ as } \zeta \to \alpha, \\ W(\zeta) &\sim -\frac{iLU}{2\pi} \log(\zeta - \beta) \text{ as } \zeta \to \beta. \end{aligned} \tag{30}$$

C. The function *dw/dz*

Once again, Bernoulli's theorem implies that

$$\left| \frac{dw}{dz} \right| = \text{constant}, \quad \text{on } |\zeta| = \rho, 1. \tag{31}$$

From an analysis of the analogous point vortex problem, in both the unstaggered and staggered cases, we expect two stagnation points in the principal period window. The preimages in the annulus of these stagnation points will be denoted γ_1 and γ_2. Owing to the periodicity of the arrangement, we require dw/dz to be L-periodic.

D. Solutions in terms of circular slit mappings

In the complex ζ-plane, the logarithmic singularities (30) of $W(\zeta)$ have a physical interpretation as point vortices with circulations of equal strength but opposite sign, at $\zeta = \alpha$ and $\zeta = \beta$. This is in contrast with the case of a single row where the two point vortices at these points had identical circulations. The solution for $W(\zeta)$ can be obtained by combining results of Crowdy and Marshall[28] and Crowdy[30] (or, for a review, see Ref. [31]). The key realization is that, in the complex ζ-plane, $W(\zeta)$ is the complex potential for the flow around two objects, with equal and opposite circulations around them, and with two point vortices, having equal strength but opposite sign, in the flow at positions $\zeta = \alpha$ and $\zeta = \beta$. The result is

$$W(\zeta) = \frac{iLU}{2\pi} \log\left(\frac{\eta(\zeta, \alpha)}{\eta(\zeta, \beta)} \right) - \frac{i\Gamma}{2\pi} \log \zeta. \tag{32}$$

It can be verified that this has constant imaginary part on $|\zeta| = \rho$, 1. It also has the required behaviour (30) near $\zeta = \alpha$ and β. It changes by Γ as either of the circles $|\zeta| = \rho$, 1 is traversed in an anticlockwise sense thereby producing the required circulations around the vortices. We refer the reader to Refs. [28], [30], and [31] for more details.

Next consider the function

$$\frac{dw}{dz} = \frac{R\eta(\zeta; \gamma_1)\eta(\zeta; \gamma_2)}{\zeta}, \tag{33}$$

where R is a complex constant: it is single-valued in the annulus $\rho < |\zeta| < 1$, so it is invariant as either of the two points α and β is encircled. It is easily checked, from the properties of the circular slit map, that the function in Eq. (33) has constant modulus on $|\zeta| = \rho$, 1. It also has two

simple zeros at $\zeta = \gamma_1$ and γ_2 which are the preimages of the two stagnation points in the principal period window. The factor of ζ in the denominator is required to ensure the vortices have the right circulations around them.

In summary, the required functions are Eqs. (32) and (33). Given these, an expression for the conformal map $z(\zeta)$ follows from

$$\frac{dz}{d\zeta} = \frac{dW/d\zeta}{dw/dz}. \tag{34}$$

To derive the most convenient expression for $z(\zeta)$, it is useful to make some further analytical observations. On differentiation of the expression for $W(\zeta)$ in Eq. (32), and on use of the relations (25), it can be shown that $\zeta dW/d\zeta$ is invariant if its argument undergoes the transformation $\zeta \mapsto \rho^2\zeta$. Also, the function $\zeta dW/d\zeta$ has only poles and zeros for $\rho < |\zeta| < 1/\rho$. Another function having the same poles and zeros in this annulus and also sharing the invariance property under $\zeta \mapsto \rho^2\zeta$, is

$$\frac{P(\zeta/\gamma_1, \rho)P(\zeta\overline{\gamma_1}, \rho)P(\zeta/\gamma_2, \rho)P(\zeta\overline{\gamma_2}, \rho)}{P(\zeta/\alpha, \rho)P(\zeta\bar{\alpha}, \rho)P(\zeta/\beta, \rho)P(\zeta\bar{\beta}, \rho)}. \tag{35}$$

The aforementioned properties of Eq. (35) can be established by repeated use of the functional relations (25). It can, therefore, be argued, based on Liouville's theorem, that $\zeta dW/d\zeta$ and the function (35) are proportional. Hence,

$$\zeta \frac{dW}{d\zeta} = \frac{\tilde{R}P(\zeta/\gamma_1, \rho)P(\zeta\overline{\gamma_1}, \rho)P(\zeta/\gamma_2, \rho)P(\zeta\overline{\gamma_2}, \rho)}{P(\zeta/\alpha, \rho)P(\zeta\bar{\alpha}, \rho)P(\zeta/\beta, \rho)P(\zeta\bar{\beta}, \rho)}, \tag{36}$$

where $\tilde{R}$ is some complex constant. On substitution of Eq. (36) into Eq. (34), and on use of Eq. (33), it follows that

$$\frac{dz}{d\zeta} = \frac{BP^2(\zeta\overline{\gamma_1}, \rho)P^2(\zeta\overline{\gamma_2}, \rho)}{P(\zeta/\alpha, \rho)P(\zeta\bar{\alpha}, \rho)P(\zeta/\beta, \rho)P(\zeta\bar{\beta}, \rho)}, \tag{37}$$

for some constant B. Finally, on integration,

$$z(\zeta) = \int_{\zeta_0}^{\zeta} \left\{ \frac{BP^2(\zeta'\overline{\gamma_1}, \rho)P^2(\zeta'\overline{\gamma_2}, \rho)}{P(\zeta'/\alpha, \rho)P(\zeta'\bar{\alpha}, \rho)P(\zeta'/\beta, \rho)P(\zeta'\bar{\beta}, \rho)} \right\} d\zeta', \tag{38}$$

where ζ_0 is a constant.

The parameters $\zeta = \gamma_1$ and $\zeta = \gamma_2$ are two solutions, in the annulus $\rho < |\zeta| < 1$, of the equation

$$\frac{dW}{d\zeta} = 0, \tag{39}$$

which, on use of (32), can be written in the form

$$K(\zeta/\alpha, \rho) - K(\zeta\bar{\alpha}, \rho) - K(\zeta/\beta, \rho) + K(\zeta\bar{\beta}, \rho) = \mu, \tag{40}$$

where we introduce

$$\mu \equiv \frac{\Gamma}{LU}, \qquad K(\zeta, \rho) \equiv \frac{\zeta \partial P(\zeta, \rho)/\partial \zeta}{P(\zeta, \rho)}. \tag{41}$$

Also, since $dw/dz \to -U$ as $z \to \infty^\pm$, it is necessary that

$$\frac{R\eta(\alpha; \gamma_1)\eta(\alpha; \gamma_2)}{\alpha} = \frac{R\eta(\beta; \gamma_1)\eta(\beta; \gamma_2)}{\beta} = -U. \quad (42)$$

One of the Eq. (42) can be used to determine R, if required and this, in turn, provides the velocity field via Eq. (33).

IV. CHARACTERIZATION OF THE SOLUTIONS

The lengthscale and timescale of the problem can be set by insisting that

$$L = \Gamma = 1. \quad (43)$$

The analogous problem of a street of point vortices admits a one parameter family of equilibrium solutions for both the unstaggered and staggered cases (see Appendix B); we take this parameter to be the speed of the street U. For a hollow vortex street, we expect an additional freedom associated with the size of the hollow vortices. The parameter ρ is a natural choice for this: we, therefore, proceed to examine the solution class with ρ and U as the two free parameters.

The constant ζ_0 in the mapping (38) reflects a translational degree of freedom and determines the position of the origin in the z-plane; this can be set arbitrarily and the mapping shifted by an appropriate constant *a posteriori*.

A. Unstaggered vortex streets

Our general strategy in finding solutions is to pick U and then gradually increase ρ from zero; for small ρ, the hollow vortices are always found to be small and close to circular. It has been found that unstaggered vortex streets exist for $U \gtrsim 0.5$; this is consistent with the result for point vortex streets as indicated in Appendix B. The parameters α, β, γ_1, and γ_2 either satisfy the condition that they are all real with

$$\beta = \frac{\rho}{\alpha}, \qquad \gamma_2 = \frac{\rho}{\gamma_1}, \quad (44)$$

or, alternatively,

$$\beta = \frac{\rho}{\alpha}, \qquad \gamma_2 = \overline{\gamma_1} = \sqrt{\rho}e^{i\phi}, \quad (45)$$

with α, β, and ϕ being real parameters. With the choices (44) and (45), it can be shown that the images of the circles $|\zeta| = 1$ and $|\zeta| = \rho$ are reflections of each other about a horizontal midline between them. In either case, for a given ρ and U, two real parameters remain to be determined. One condition to determine these parameters is

$$\mathrm{Im}\left(\oint_{|\zeta|=1} \frac{dz}{d\zeta}d\zeta\right) = 0, \quad (46)$$

which is necessary if the image of $|\zeta| = 1$ is to be a closed curve. Once this is satisfied, the condition that the image of $|\zeta| = \rho$ is also a closed curve, i.e.,

$$\mathrm{Im}\left(\oint_{|\zeta|=\rho} \frac{dz}{d\zeta}d\zeta\right) = 0, \quad (47)$$

follows automatically because of the symmetry between the two vortices resulting from the choices (44) or (45). It must

also be arranged that γ_1 is a zero of Eq. (40) for the given choice of U and this is the second real condition that will determine the final unknown parameter. The value of B is found, *a posteriori*, by insisting that the residue of $dz/d\zeta$ at $\zeta = \alpha$ is $-iL/(2\pi)$, as required by Eq. (20). This condition takes the form

$$\frac{iL}{2\pi} = \frac{B\alpha P^2(\alpha\overline{\gamma_1}, \rho)P^2(\alpha\overline{\gamma_2}, \rho)}{\hat{P}(1, \rho)P(|\alpha|^2, \rho)P(\alpha/\beta, \rho)P(\alpha\bar{\beta}, \rho)}, \quad (48)$$

where

$$\hat{P}(\zeta, \rho) \equiv \frac{P(\zeta, \rho)}{(1 - \zeta)} = \prod_{k=1}^{\infty}(1 - \rho^{2k}\zeta)(1 - \rho^{2k}\zeta^{-1}). \quad (49)$$

We are principally interested here in the hollow vortex shapes. If the velocity field in a typical period window is required, it is necessary to make a particular choice of branch cut between points α and β that would mark the straight vertical edges of the period window. To find such branch cuts between α and β, it is necessary to solve an ordinary differential equation for ζ as a function of z obtained by differentiating the equation $\mathrm{Re}(z(\zeta)) = \text{constant}$ and then making use of the expression (37) for $dz/d\zeta$.

For each fixed value of $0.5 \lesssim U < 0.5773502693$, there is a critical value of ρ below which all parameters are real and satisfy Eq. (44). Figure 4 shows a schematic of the locations of parameters α, β, γ_1, and γ_2 in this case. Then, at the critical ρ, the zeros γ_1 and γ_2 merge on the real axis at $\sqrt{\rho}$ and, for higher ρ, γ_1, and γ_2 become a complex conjugate pair sitting on the circle $|\zeta| = \sqrt{\rho}$. Figure 4 also shows typical positions of α, β, γ_1, and γ_2 in this second case. A graph of the critical value of ρ as a function of U is shown in Figure 5. This transition of the zeros γ_1 and γ_2 off the real axis onto the circle $|\zeta| = \sqrt{\rho}$ has a physical significance: the two stagnation points on the edge of each period window move off those edges onto the real axis. For $U > 0.5773502693$, the parameters α, β, γ_1, and γ_2 always satisfy Eq. (45) and, therefore, the stagnation points in the co-travelling frame for these solutions are always on the real axis.

Figure 6 shows three periods of typical unstaggered vortex streets for $U = 0.6$ and $U = 0.8$. The maximum area of the vortices in the street decreases as U increases; this is consistent with the results shown later in Figure 11. These unstaggered street solutions can be viewed as a generalization of the classical hollow vortex pair solutions due to Pocklington[22] to the case of a singly periodic array of such vortex pairs all travelling in the same direction. It is reassuring that the vortex shapes in these streets closely resemble those found by Pocklington.[22] They exhibit maximum area configurations in which each vortex has a long flattened face along the region of the vortex sheet boundaries which are closest together.

B. Staggered vortex streets

More physically relevant is the case of staggered vortex streets. These are found to exist for $0 < U \lesssim 0.5$ which is
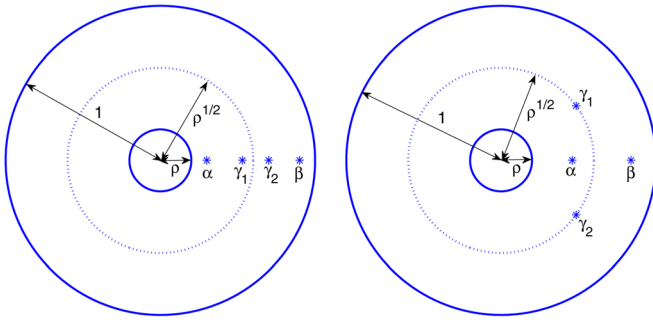
FIG. 4. (Color online) The distribution of parameters α, β, γ_1, and γ_2 in the two cases (44) and (45) for the unstaggered street solutions. For fixed $0.5 \lesssim U < 0.5773502693$, there is a critical ρ for which $\gamma_1 = \sqrt{\rho} = \gamma_2$ represents a transition between the two situations shown.

again consistent with the point vortex street result in Appendix B. In this case, all parameters α, β, γ_1, and γ_2 are real. In contrast to Eq. (44), it is now found that

$$\beta = -\frac{\rho}{\alpha}, \qquad \gamma_2 = -\frac{\rho}{\gamma_1}. \qquad (50)$$

These relations hold for all staggered street solutions we computed. Once again, for given ρ and U, the unknown parameters are determined by ensuring that the image of $|\zeta| = 1$ is a closed curve and that γ_1 is a zero of Eq. (40).

Figure 7 shows three periods of typical staggered vortex streets for $U = 0.2$ and $U = 0.4$. As its size increases, each vortex adopts a very distinctive triangular shape with two flattened faces along the regions of the vortex sheet boundary closest to their nearest neighbours. These triangular shapes are reminiscent of the photographs of certain staggered vortex streets shown, for example, in Van Dyke's album of fluid motion.[32] For a fixed U, it is found that ρ can be increased up to some limiting value with no apparent singularity in the vortex shape or loss of univalence of the conformal mapping. Our staggered street solutions are the hollow vortex analogues of the staggered streets of vortex patches found numerically by Saffman and Schatzman.[15] It is instructive to compare our solutions with theirs and to reparametrize our
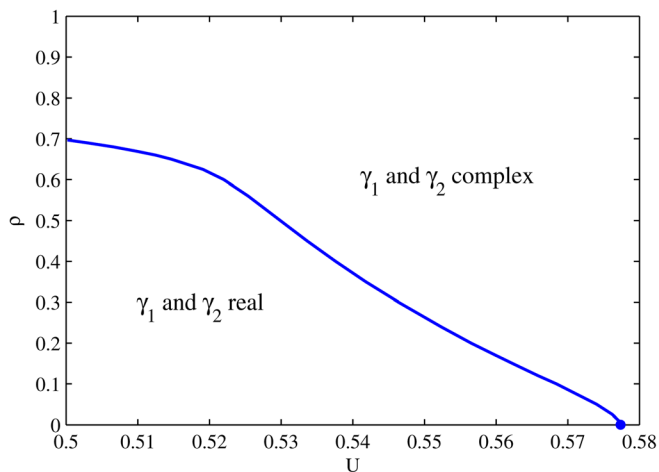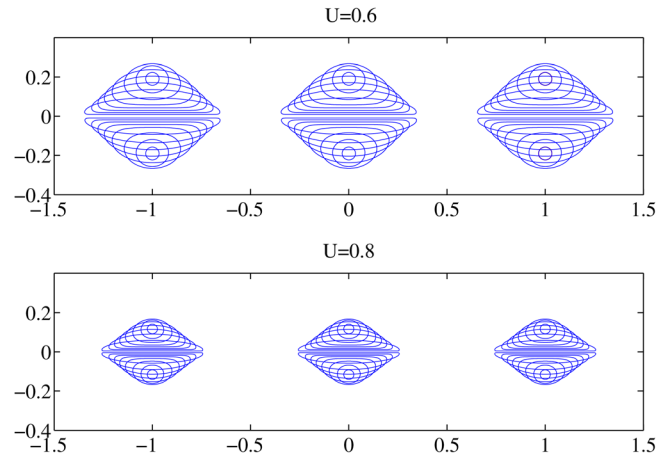

FIG. 6. (Color online) Three periods of unstaggered vortex streets with speeds $U = 0.6$ and $U = 0.8$ and hollow vortices of different areas (the different solutions have been superposed). The maximum possible area of the hollow vortices in the street decreases as U increases.

solutions to emulate their presentation. Figure 2 of Saffman and Schatzman[15] shows the speed U against the area of the vortex patches making up the street for several fixed aspect ratios κ; their Figure 3 is a graph of the quantity,

$$D = -\frac{1}{2}\mathrm{Im}\int_{-i\infty}^{i\infty}(u - U - iv)^2 dz, \qquad (51)$$

FIG. 5. (Color online) Graph showing the critical value of ρ, for each U, at which the parameters for unstaggered vortex streets transition from satisfying Eq. (44) to satisfying Eq. (45).
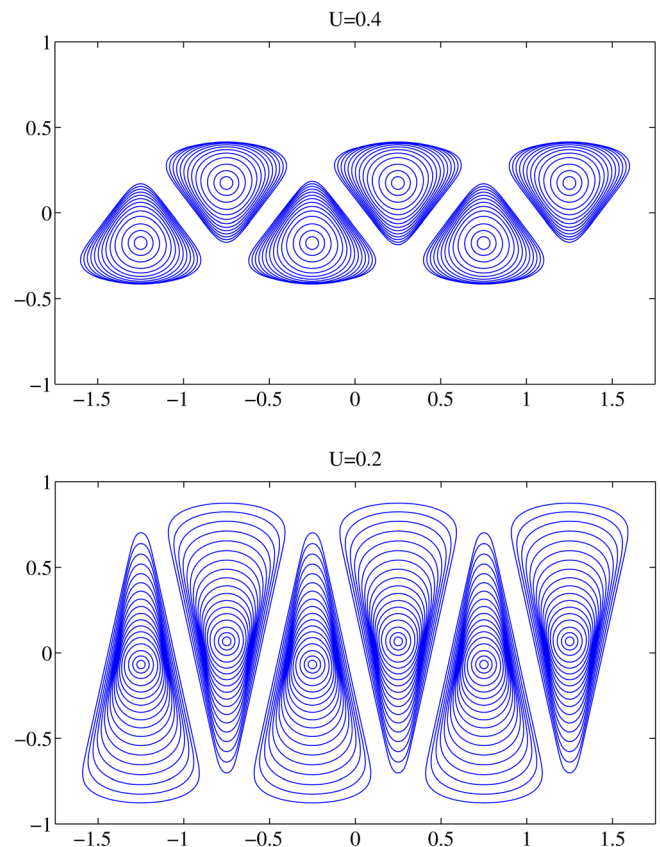
FIG. 7. (Color online) Three periods of typical staggered vortex streets with $U = 0.2$ and $U = 0.4$ and hollow vortices of different areas (the different solutions have been superposed).

against vortex patch area for the same choices of κ. Physically, D is essentially the momentum flux of the fluid in the streamwise direction with the contribution from the vortices themselves omitted. In evaluating D from Eq. (51), any contour joining $-i\infty$ to $i\infty$ that does not cross either of the vortices is acceptable. Introduce the aspect ratio of the street

$$\kappa = \frac{h}{L}, \qquad (52)$$

where h is the vertical separation of the centroids of the vortices in the two rows. The latter quantity is readily computed from the analytical expressions for the solutions. Figure 8 shows graphs of U against the area of the hollow vortices for various values of κ. We find that there is a critical value of κ, somewhere between $\kappa = 0.33$ and $\kappa = 0.35$, where the qualitative behaviour of these graphs changes dramatically. For $\kappa \leq 0.33$, the speed U of the street for a given vortex area is unique; but, for $\kappa \geq 0.35$, the U graphs turn around implying non-uniqueness of the street solutions for given aspect ratio and vortex area. To get an idea of how different the two possible solutions are, Figure 9 shows two different vortex streets, of aspect ratio $\kappa = 0.4$, with vortex area equal to 0.175. The street in which the vortices are more extended in the streamwise direction travels with the greater speed. Saffman and Schatzman[15] find exactly the same qualitative behaviour for their vortex patch streets; even more, they state the critical aspect ratio to be $\kappa \approx 0.36$, which is remarkably close to the value found here. It is intriguing that a similar critical aspect ratio arises even though the inviscid vortex models used are so different. Given that it has arisen in two distinct finite-area vortex models of a staggered vortex street, it is natural to ask whether this critical aspect ratio of approximately 0.34–0.36 has any special physical significance; so far, we are unable to offer an interpretation and it is perhaps just a coincidence.

Figure 10 shows a graph of the quantity D against vortex area for various choices of κ and, again, it is qualitatively similar to Figure 3 of Saffman and Schatzman.[15] The latter authors also include graphs of excess energy T against vortex
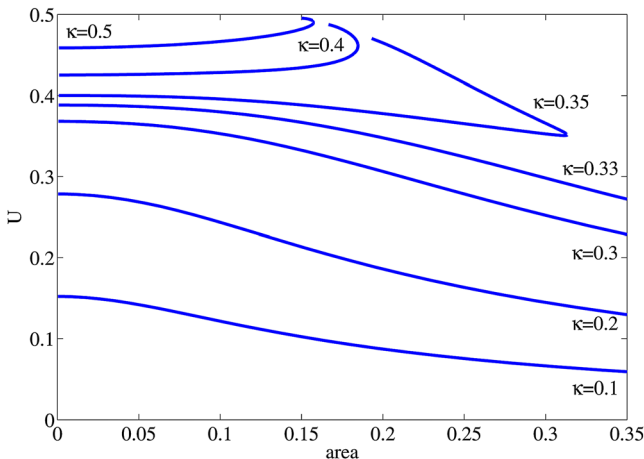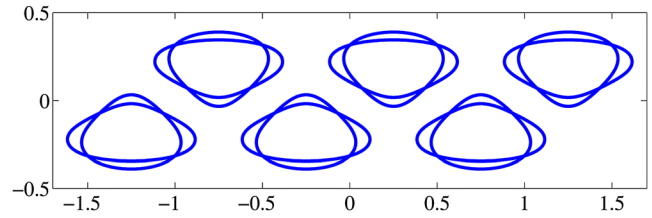

FIG. 9. (Color online) Non-uniqueness of solutions: two different vortex streets are superposed, each comprising vortices of area 0.175 and with aspect ratio $\kappa = 0.4$. The street with vortices that are more extended in the streamwise direction travels faster ($U = 0.4817$, compared to $U = 0.4437$) but has a lower value of the momentum flux D.

area for their streets of vortex patches; we have not computed T for the hollow vortex solutions found here, but we expect this to qualitatively resemble Figure 4 of Ref. 15.

The nature of the limiting hollow vortex shapes is of interest and, here, the solution branches are terminated when the Newton iteration to find parameters satisfying the required conditions no longer converges. It appears that the solution branches of Saffman and Schatzman[15] terminate for similar reasons of numerical failure to find a continuation of the branch. The shape of the hollow vortices at the points where the Newton iteration fails do not exhibit any corners, cusps, or other singularities, or indeed any loss of univalence. It is possible that the solution branches continue into a class of non symmetric solutions where the vortices in each row do not have the same shape, but this has not been investigated here. Saffman and Schatzman[15] comment on the structure of their solution branches from the point of view of variational principles. The general matter of variational arguments applied to steady vortical equilibria has lately been reappraised, and clarified, by Luzzatto-Fegiz and Williamson.[37] Given that the solutions here are available in closed mathematical form, it would be of interest to examine to what extent that approach can throw light on the structure, and stability, of this solution class.

A final observation is that, for both staggered and unstaggered streets, for a fixed U, there is a maximum admissible area of the hollow vortices in the street. A graph of this maximum area against U is shown in Figure 11; it shows the
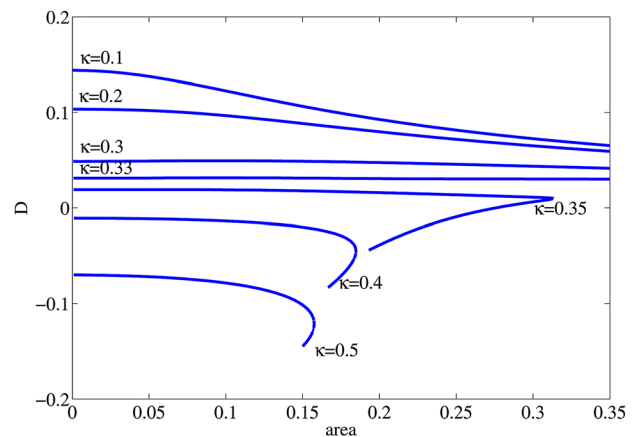

FIG. 8. (Color online) Graphs of U against area for several fixed aspect ratios κ. This figure should be compared with Figure 2 of Saffman and Schatzman.[15]

FIG. 10. (Color online) Graphs of D against area for different aspect ratios κ. This figure should be compared with Figure 3 of Saffman and Schatzman.[15]
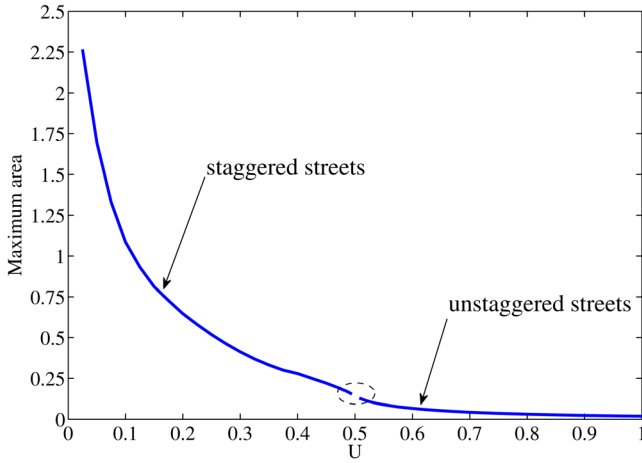
FIG. 11. (Color online) A graph of the maximum area of the hollow vortices in a street as a function of the speed of the street U, including both unstaggered and staggered varieties. It is difficult to find parameters for $U \approx 0.5$, but the graph appears to be a near-continuous function.

interesting feature that, even though it includes both staggered and unstaggered vortex streets, the curve appears to be a very nearly continuous one, with the maximum area of staggered vortex streets with $U \to 0.5^-$ appearing to nearly "match up" with the maximum area for unstaggered vortex streets with $U \to 0.5^+$. It is difficult to numerically determine parameters satisfying all the necessary conditions, for either staggered or unstaggered streets, when U is very close to $U = 0.5$ so there is a small "gap" in the graph in this neighbourhood. Saffman and Schatzman[15] found similar regions of parameter space where convergence of their numerical method was hard to achieve.

V. DISCUSSION

A class of exact solutions for both unstaggered and staggered streets of hollow vortices in relative equilibrium has been presented. The solutions can be written down in closed form. A characterization of their properties has been given. It is worth remarking that, like the co-travelling hollow vortex pair solution of Pocklington,[22] the new solutions found here can, in principle, be rewritten in terms of elliptic functions, but this is not necessary, and we find no technical advantage in this.

It has been found that the aspect ratio of $\kappa \approx 0.34$–0.36 shares a particular significance in both the inviscid vortex patch and hollow vortex models of a staggered street; in both models it is the aspect ratio around which a "cross-over" occurs between the existence of equilibria where, in one case, as the vortices grow in size they impinge on the vortices in the other row while, in the second case, as the vortex size increases vortices in each row tend to merge with their neighbours (thereby tending to the situation comprising two continuous vortex layers with opposite signed vorticity).

We have focussed here on the construction of the equilibrium solutions but it is important to ascertain their linear stability properties and this is currently under investigation. Llewellyn Smith and Crowdy[33] have recently presented new

results on the structure and stability of certain hollow vortex equilibria, including a full Floquet analysis of the linear stability properties of the single hollow vortex row of Baker et al.[19] It should be possible to adapt that analysis to the vortex street solutions herein. The recent ideas of Luzzatto-Fegiz and Williamson[37] may also be able to throw some light on stability matters.

Saffman and Schatzman[34] have used their numerical solutions for streets of finite-area vortex patches to propose an inviscid model of the vortex street wake behind a cylinder. They invoked conservation of momentum, energy, and vorticity to link parameters associated with the near-field wake to characteristics of their steady downstream vortex street solutions. In principle, an analogous model involving the hollow vortex street solutions found here can be formulated and a comparison of the models is an interesting topic for investigation. Given that the solutions here are available in analytical form, a matching of parameters is expected to be easier to carry out than for the patch model of Ref. 34.

The hollow vortex model provides a theoretical gateway to the investigation of the effects of compressibility on vortex structures and such effects have already been studied both for the Pocklington vortex pair,[35,36] as well as the single hollow vortex row.[21] It would be of great interest, for example to the aerospace industry, to investigate compressibility effects in von Kármán vortex street structures and the exact solutions found here are likely to provide a convenient starting point for any such theoretical investigations.

ACKNOWLEDGMENTS

APPENDIX A: RELATION TO BAKER, SAFFMAN AND SHEFFIELD

The conformal map (19) is

$$z(\zeta) = \frac{L}{\pi} \left(\tan^{-1}(\zeta/a) - a^2 \tan^{-1}(a\zeta) \right), \qquad \text{(A1)}$$

where we have taken $z_0 = 0$. Let $\zeta = e^{i\phi}$, with $0 \leq \phi < 2\pi$, so that

$$z(\phi) = x(\phi) + iy(\phi) = \frac{L}{\pi} \left(\tan^{-1}(e^{i\phi}/a) - a^2 \tan^{-1}(ae^{i\phi}) \right). \qquad \text{(A2)}$$

On use of the identity,

$$\tan^{-1}(Z) = \frac{i}{2}\log\left(\frac{i+Z}{i-Z}\right),$$

(A2) becomes

$$x(\phi) + iy(\phi) = \frac{L}{\pi}\log\left(\left(\frac{ai+e^{i\phi}}{ai-e^{i\phi}}\right)^{i/2}\left(\frac{i-ae^{i\phi}}{i+ae^{i\phi}}\right)^{a^2i/2}\right).$$

(A3)

Let

$$\frac{ai+e^{i\phi}}{ai-e^{i\phi}} = R_1 e^{i\Theta_1}, \quad \frac{i-ae^{i\phi}}{i+ae^{i\phi}} = R_2 e^{i\Theta_2},$$

where the real numbers R_1, R_2, Θ_1, and Θ_2 can be found. Then,

$$x(\phi) + iy(\phi) = \frac{iL}{2\pi}\left(\log(R_1 e^{i\Theta_1}) + a^2\log(R_2 e^{i\Theta_2})\right),$$
$$= \frac{L}{2\pi}\left(-\Theta_1 - a^2\Theta_2 + i(\log R_1 + a^2\log R_2)\right).$$

(A4)

Thus,

$$x(\phi) = -\frac{L}{2\pi}(\Theta_1 + a^2\Theta_2),$$
$$y(\phi) = \frac{L}{2\pi}(\log R_1 + a^2\log R_2).$$

(A5)

From (17), we have

$$\frac{dw}{dz} = \frac{iU\zeta}{a}.$$

(A6)

Baker et al.[19] define quantity

$$R = \frac{U_\infty}{q_0}.$$

(A7)

In our notation, $U_\infty = U$, and

$$q_0 = \left|\frac{dw}{dz}\right|_{|\zeta|=1} = \frac{U}{a}.$$

(A8)

Hence, we identify that

$$R = a.$$

(A9)

After some algebra, it can be shown that

$$R_1 = \frac{1 + 2R\sin\phi + R^2}{((1+R^2)^2 - 4R^2\sin^2\phi)^{1/2}} = \frac{1}{R_2},$$
$$\Theta_1 = \tan^{-1}\left(\frac{2R\cos\phi}{1-R^2}\right) = \Theta_2,$$

(A10)

and so, on use of Eq. (A9), Eq. (A5) becomes

$$x(\phi) = -\frac{L}{2\pi}(1+R^2)\tan^{-1}\left(\frac{2R\cos\phi}{1-R^2}\right),$$
$$y(\phi) = \frac{L}{2\pi}(1-R^2)\log\left(\frac{1 + 2R\sin\phi + R^2}{((1+R^2)^2 - 4R^2\sin^2\phi)^{1/2}}\right).$$

(A11)

The parametric equations for the free surface as given by Baker et al.[19] are

$$x(\lambda) = \frac{L}{2\pi}(1+R^2)\sin^{-1}\left(\frac{2R\sin\lambda}{1+R^2}\right),$$
$$y(\lambda) = \frac{L}{2\pi}(1-R^2)\sinh^{-1}\left(\frac{2R\cos\lambda}{1-R^2}\right).$$

(A12)

On use of the identities,

$$\sin(\tan^{-1}Z) = \frac{Z}{(1+Z^2)^{1/2}}, \quad \sinh(\log Z) = \frac{1}{2}\left(Z - \frac{1}{Z}\right),$$

(A13)

and with the identification of parameters λ and ϕ given by

$$\cos\lambda = \frac{(1-R^2)\sin\phi}{((1+R^2)^2 - 4R^2\sin^2\phi)^{1/2}},$$
$$\sin\lambda = -\frac{(1+R^2)\cos\phi}{((1+R^2)^2 - 4R^2\sin^2\phi)^{1/2}},$$

(A14)

we find

$$-\tan^{-1}\left(\frac{2R\cos\phi}{1-R^2}\right) = \sin^{-1}\left(\frac{2R\sin\lambda}{1+R^2}\right)$$

(A15)

and

$$\log\left(\frac{1 + 2R\sin\phi + R^2}{((1+R^2)^2 - 4R^2\sin^2\phi)^{1/2}}\right) = \sinh^{-1}\left(\frac{2R\cos\lambda}{1-R^2}\right),$$

(A16)

which shows that Eqs. (A11) and (A12) are identical.

APPENDIX B: POINT VORTEX STREETS

In this section, we include some details of the analysis for constructing steady point vortex streets. We focus on staggered streets, but the unstaggered case involves only minor changes in detail. Consider two staggered rows of point vortices with a top row comprising point vortices all of circulation Γ and a lower row comprising point vortices all of circulation $-\Gamma$. Suppose the configuration moves, without change of form, with speed U. The vortices in both rows are assumed to be separated by L. The complex potential in a frame co-travelling with the configuration is

$$w(z) = -Uz - \frac{i\Gamma}{2\pi}\log\sin\left(\frac{\pi(z-c)}{L}\right)$$
$$+ \frac{i\Gamma}{2\pi}\log\sin\left(\frac{\pi(z+c)}{L}\right),$$

(B1)

where $\pm c$ are such that $-L/2 < \text{Re}[\pm c] < L/2$. The complex velocity is

$$\frac{dw}{dz} = -U - \frac{i\Gamma}{2L}\cot\left(\frac{\pi(z-c)}{L}\right) + \frac{i\Gamma}{2L}\cot\left(\frac{\pi(z+c)}{L}\right).$$

(B2)

The condition that the vortex at $z = c$ is stationary (and, hence, by periodicity, all the other vortices in this row) is

$$-U + \frac{i\Gamma}{2L}\cot\left(\frac{2\pi c}{L}\right) = 0. \tag{B3}$$

By symmetry, it is easy to show that the same condition ensures that the vortices in the lower row are also stationary. Thus

$$\tan\left(\frac{2\pi c}{L}\right) = \frac{i\Gamma}{2LU}. \tag{B4}$$

On use of the identity,

$$\tan(X + iY) = \frac{\tan X \, \text{sech}^2 Y}{1 + \tan^2 X \tanh^2 Y} + \frac{i \tanh Y \, \text{sec}^2 X}{1 + \tan^2 X \tanh^2 Y}, \tag{B5}$$

it is clear that we require

$$\frac{2\pi c}{L} = \frac{\pi}{2} + iY, \tag{B6}$$

where

$$\coth Y = \frac{\Gamma}{2LU}. \tag{B7}$$

Thus, we must have

$$c = \frac{L}{4} + \frac{iL}{2\pi}\coth^{-1}\left(\frac{\Gamma}{2LU}\right). \tag{B8}$$

It is also clear that, if $\Gamma = 1 = L$, then staggered point vortex street solutions only exist provided that $0 < U < 0.5$. For unstaggered streets, a similar analysis reveals that point vortex equilibria exist provided $U > 0.5$.

[1]P. G. Saffman, *Vortex Dynamics* (Cambridge University Press, Cambridge, 1992).

[2]C. H. K. Williamson, "Vortex dynamics in the cylinder wake," Ann. Rev. Fluid Mech. **28**, 477 (1996).

[3]T. von Kármán and H. Rubach, "On the mechanism of resistance in fluids," Phys. Z. **13**, 49 (1912) (in German).

[4]T. von Kármán, *Collected Works of Theodore von Kármán* (Butterworths, London, 1956), Vol. 1.

[5]K. P. Chopra and L. F. Hubert, "Mesoscale eddies in wakes of islands," J. Atmos. Sci. **45**, 2961 (1988).

[6]R. E. Thomson, J. F. R. Gower, N. W. Bowker, "Vortex streets in the wake of the Aleutian islands," Mon. Weather Rev. **105**, 873 (1977).

[7]G. S. Young and J. Zawislak, "An observational study of vortex spacing in island wake vortex streets," Mon. Weather Rev. **134**, 2285 (2006).

[8]M. Shao, H. Hu, M. Li, H. Ban, M. Wang, and J. Jiang, "Kármán vortex street assisted patterning in the growth of silicon nanowires," Chem. Commun. **8**, 793 (2007).

[9]K. Sasaki, N. Suzuki, and H. Saito, "Bénard-von Kármán vortex street in a Bose-Einstein condensate," Phys. Rev. Lett. **104**, 150404 (2010).

[10]K. Sasaki, N. Suzuki, H. Saito, "Dynamics of bubbles in a two-component Bose-Einstein condensate," Phys. Rev. A **83**, 033602 (2011).

[11]J. C. Liao, D. N. Beal, G. V. Lauder, and M. S. Triantafyllou, "The Kármán gait: novel body kinematics of rainbow trout swimming in a vortex street," J. Exp. Biol. **206**, 1059 (2003).

[12]R. W. Whittlesey, S. C. Liska, and J. O. Dabiri, "Fish schooling as a basis for vertical-axis wind turbine farm design," Bioinspiration and Biomimetics **5**, 035005 (2010), http://iopscience.iop.org/1748-3190/5/3/035005/.

[13]S. G. Hooker, "On the action of viscosity in increasing the spacing ratio of a vortex street," Proc. Roy. Soc. London, Ser. A **154**, 67 (1936).

[14]J. W. Schaefer and S. Eskinazi, "An analysis of the vortex street generated in viscous fluid," J. Fluid Mech. **6**, 241 (1959).

[15]P. G. Saffman and J. C. Schatzman, "Properties of a vortex street of finite vortices," SIAM (Soc. Ind. Appl. Math.) J. Sci. Stat. Comput. **2**(3), 285 (1981).

[16]P. G. Saffman and J. C. Schatzman, "Stability of a vortex street of finite vortices," J. Fluid Mech. **117**, 171 (1982).

[17]S. Kida, "Stabilizing effects of finite core on Kármán vortex street," J. Fluid Mech. **122**, 487 (1982).

[18]D. I. Meiron, P. G. Saffman, and J. C. Schatzman, "The linear two-dimensional stability of inviscid vortex streets of finite-cored vortices," J. Fluid Mech. **147**, 187 (1984).

[19]G. R. Baker, P. G. Saffman, and J. S. Sheffield, "Structure of a linear array of hollow vortices of finite cross-section," J. Fluid Mech. **74**, 469 (1976).

[20]G. R. Baker, "Energetics of a linear array of hollow vortices of finite cross-section," J. Fluid Mech. **99**, 97 (1980).

[21]K. Ardalan, D. I. Meiron, and D. I. Pullin, "Steady compressible vortex flows: the hollow-core vortex array," J. Fluid Mech. **301**, 1 (1995).

[22]H. C. Pocklington, "The configuration of a pair of equal and opposite hollow straight vortices of finite cross-section, moving steadily through fluid," Proc. Cambridge Philos. Soc. **8**, 178 (1895).

[23]H. Telib and L. Zannetti, "Hollow wakes past arbitrarily shaped obstacles," J. Fluid Mech. **669**, 214 (2011).

[24]P. G. Saffman, "Perspectives in vortex dynamics," Lect. Notes Phys. **320**, 91 (1988).

[25]G. K. Batchelor, *An Introduction to Fluid Dynamics* (Cambridge University Press, Cambridge, 1967).

[26]L. Milne-Thomson, *Theoretical Hydrodynamics* (Dover, New York, 1996).

[27]L. I. Sedov, *Two-Dimensional Problems in Hydrodynamics and Aerodynamics* (Wiley, New York, 1965).

[28]D. G. Crowdy and J. S. Marshall, "Analytical formulae for the Kirchhoff-Routh path function in multiply connected domains," Proc. Roy. Soc. London, Ser. A **461**, 2477 (2005).

[29]D. G. Crowdy and J. S. Marshall, "Conformal mappings between canonical multiply connected domains," Comput. Methods Funct. Theory **6**(1), 59 (2006), http://www.heldermann.de/CMF/CMF06/CMF061/cmf06006.htm.

[30]D. G. Crowdy, "Calculating the lift on a finite stack of cylindrical aerofoils," Proc. Roy. Soc. London, Ser. A **462**, 1387 (2006).

[31]D. G. Crowdy, "A new calculus for two-dimensional vortex dynamics," Theor. Comput. Fluid Dyn. **24**, 9 (2010).

[32]M. Van Dyke, *An Album of Fluid Motion* (Parabolic, Stanford, 1982).

[33]S. Llewellyn Smith and D. G. Crowdy, "Structure and stability of hollow vortex equilibria," J. Fluid Mech. (in press).

[34]P. G. Saffman and J. C. Schatzman, "An inviscid model for the vortex-street wake," J. Fluid Mech. **122**, 467 (1982).

[35]D.W. Moore and D. I. Pullin, "The compressible vortex pair," J. Fluid Mech. **185**, 171 (1987).

[36]F.G. Leppington, "The field due to a pair of line vortices in a compressible fluid," J. Fluid Mech. **559**, 45 (2006).

[37]P. Luzzatto-Fegiz and C. H. K. Williamson, "Stability of conservative flows and new steady-fluid solutions from bifurcation diagrams exploiting a variational argument," Phys. Rev. Lett. **104**, 044504 (2010).